

Study on Application of UV-Processed Molecular Alignment in Liquid Crystal Devices

(液晶素子における UV 処理された分子配向膜の応用に関する研究)

A thesis submitted to the
Graduate School of Engineering of
Nagaoka University of Technology in partial fulfillment
of the requirements for the degree of
Doctor of Engineering

by

Jais Bin Lias
06539591

Academic adviser
Associate Prof. Dr. Munehiro Kimura

Department of Electrical Engineering
Nagaoka University of Technology
2011

Abstract

Photoalignment technique in liquid crystal devices (LCDs) fabrication processes is classified into a non-contact process which provides an anisotropy in liquid crystal (LC) alignment layer by exposing ultra violet (UV) light. The greatest benefit for using this technique is to avoid electrostatic charges and impurities on the substrate. Moreover, photoalignment can realize the structures which has the required liquid crystal director azimuth with the selected area of the cell, thus viewing angle characteristics can be improved by the pixel dividing. In this study, the photoalignment technique was applied to the fabrication of a bistable type LCD and polymer-stabilized blue phase (PSBP) LCD.

Most liquid crystal devices are monostable, which possesses only one possible state in absence of field. They requires continuous voltage application and frequent image refreshment, which is the cause of the energy consumption and limits the multiplexability. In other word, monostable devices have no intrinsic pixel memory and they need an active matrix or other external storage elements to obtain high multiplexing levels. Bistable type LCD have two (or more) stable states. Once an image displayed, the director state in each pixels is memorized for a long time, ranging from seconds up to years, until when the new image is overwritten. This intrinsic memory capability is a peculiar advantage of the bistable type LCD, provides a potential to reduce the power consumption, especially for the specific application which is unnecessary frequent update. In this study, to fabricate a bistable LCD (BLCD) by using unpolarized UV light irradiation, single-step laser patterning to photoalignment layer was proposed. Bistability can be achieved by two equilibrium configurations of LC director profile which is induced by a periodically patterned alignment layer on a substrate. The patterns were formed by stripes of alternating random planar and homeotropic anchoring in the order of 0.5 μm . In this work, two possible configurations of bistable LCD that can be obtained by combining a micropatterned surface formed with alternating random-planar- and homeotropic-alignment with planar- or homeotropic-alignment surfaces were proposed. The alignment properties of the two proposed BLCD models such as twisted angle, pretilt angle and its microscopic switching behavior and memory effect were investigated and determined. It was assumed that the formation of the two bulk orientational states will depend on the degree of depolarization of the laser light, the stripe periodicity and the effective anchoring strength of the patterned surface.

Recently, blue phase (BP) liquid crystal (LC) has attracted the attention of many researchers because of its exotic structures and properties. BP with a structure of self-assembled three-dimensional cubic structure formed by double-twisted arranged LC cylinders is usually observed in a cooling process from isotropic to chiral nematic (N*) phase LC. Such a molecular arrangement exhibits an optical isotropy, selective reflection to circular polarized light, a reflective band switched by external fields, and microsecond response. These characteristics show some potential applications of BP such as large-screen flat panel displays and tuneable photonic band gap devices. The very narrow stable temperature range of the BP, however, typically a few Kelvin, is a serious problem for device applications. Although, much effort has been made to expand the narrow temperature range of the BP, Kikuchi *et al.* firstly reported that the temperature range of the BP can be expanded over 60 °C by adding a small quantity of precursor polymers within the BP materials, referred to as a polymer-stabilized blue phase (PSBP).

To realize a fast response LCD, PSBP LCD was successfully fabricated by applying the UV photoalignment technique to expand the temperature range of blue phase (BP). As a coupling coefficient, the polar anchoring strength between the BP LC and the diacrylate type polymer was evaluated by means of the oblique incidence transmission spectroscopic ellipsometry using two methods which are SOITE method and Hung's method. In the two methods, different type of LC materials and chiral dopant were employed. As a result, the polar anchoring strength measured with SOITE and Hung's methods were determined in the order of 10^{-4} J/m². The polar anchoring strength also compared with the other materials which was used for polymer dispersed LCD. We found that the host BPLC materials and the diacrylate-type polymer in a PSBP LC having vertical (homeotropic) alignment. It is assumed that the strong polar anchoring strength between the BPLC and the diacrylate-type polymer allows the PSBP LC to maintain and stabilize its structure. Thus, the BP temperature range can be broadened by adopting a diacrylate-type polymer into host BPLC materials. The finding that the polar anchoring strength is relatively high offers an important insight with which to understand and optimize the polymer stabilization of BP.

Table of Contents

Chapter 1	1
Introduction	1
1.1. History of Liquid Crystals	1
1.2. Research Background	3
1.3. Objectives of the Investigation	5
1.4. Outline of This Thesis	6
Chapter 2	8
Physical Properties of Liquid Crystals	8
2.1. Introduction	8
2.2. Thermotropic, Polymeric and Lyotropic Liquid Crystals	9
2.2.1. Thermotropic Liquid Crystal	9
2.2.1.1. Nematic and Cholesteric Phases	10
2.2.1.2. Smetic A and Smetic C Phases	12
2.2.2. Polymer Liquid Crystal	12
2.3. Properties of Liquid Crystals	13
2.3.1. Dielectric Constant	13
2.3.2. Refractive Index	14
2.3.3. Elastic Constants	14
2.3.4. Viscosity	16
Chapter 3	19
Optics of Liquid Crystals	19
3.1. Introduction	19
3.2. Light propagation in an Isotropic Medium	19
3.3. Light propagation in an Anisotropic Medium	22
3.4. Jones Matrix	26
3.5. 4×4 Matrix Method	29
3.6. Light transmission and reflection by an anisotropic plate sandwiched between isotropic media	35

Chapter 4	40
Bistable Liquid Crystal Technologies	40
4.1. Introduction	40
4.2. Principles of Operation, Advantages and Limitations	40
4.2.1. Bistable Cholesteric Display	40
4.2.2. Surface Stabilized Ferroelectric Liquid Crystal (SSFLC) Display	41
4.2.3. Bulk Bistable Twisted Nematic (360° BTN) Display	42
4.2.4. Surface Nematic Bistability	43
4.2.4.1. Zenithal Bistable Display (ZBD)	44
4.2.4.2. Surface Controlled Bistable Nematic (<i>BiNem</i>) Display	45
4.3. Present State and Expected Future of the Bistable LC Technologies	46
Chapter 5	49
Liquid Crystalline Blue Phases	49
Chapter 6	58
Investigation of Liquid Crystal Alignment on Patterned-Alignment Films Processed by UV Light	58
6.1. Introduction	58
6.2. Liquid Crystals Alignment Method	60
6.2.1. Rubbing Method	60
6.2.1.1. Definition	60
6.2.2. Photoalignment Method	62
6.3. Bistable Switching Models	63
6.4. Experiment	64
6.4.1. Orientation Confirmation of the Twisted-Homogeneous Bistable and Bistable HAN Cells	65
6.4.2. Measurement of the Twisted Angle of the Twisted-Homogeneous Bistable Cell	66
6.4.3. Measurement of the Pretilt Angle of the Twisted-Homogeneous Bistable Cells	67
6.4.4. Switching Experiment of the Twisted-Homogeneous Bistable Cell	68
6.5. Result and Discussion	68

6.5.1. Orientation Confirmation of the Twisted-Homogeneous Bistable and Bistable HAN Cells	68
6.5.2. Measurement of the Twisted Angle of the Twisted-Homogeneous Bistable Cell	70
6.5.3. Measurement of the Pretilt Angle of the Twisted-Homogeneous Bistable Cell	71
6.5.4. Switching Experiment of the Twisted-Homogeneous Bistable Cell	72
6.5.5. Effect of the Pattern Pitch	74
6.6. Conclusion	75
Chapter 7	78
Determination of Polar Anchoring Strength for Polymer-Stabilized Blue Phase Liquid Crystal Devices Processed by UV Light - SOITE Method	78
7.1. Introduction	78
7.2. Experimental Methods	79
7.2.1. Observation of Polymer-Stabilized Blue Phase	79
7.2.2. Measurement of Polar Anchoring Energy Coefficient A_0 by SOITE Method	80
7.3. Result and Discussion	83
7.3.1. Observation of Polymer-Stabilized Blue Phase	83
7.3.2. Measurement of Polar Anchoring Energy Coefficient A_0 by SOITE Method	84
7.4. Conclusion	87
Chapter 8	89
Determination of Polar Anchoring Strength for Polymer-Stabilized Blue Phase Liquid Crystal Devices Processed by UV Light – Hung’s Method	89
8.1. Introduction	89
8.2. Experimental Methods	90
8.2.1. Observation of Polymer-Stabilized Blue Phase	90
8.2.2. Measurement of Refractive Indices and the Splay Elastic Constants, K_{11} and Bend Elastic Constants, K_{33}	92
8.2.3. Measurement of Polar Anchoring Strength W_d by Hung’s Method	

K_{11} and Bend Elastic Constants, K_{33}	93
8.3. Result and Discussion	99
8.4. Conclusion	103
Chapter 9	106
Conclusions	106
Publication and Research Activities	108
Acknowledgement	110

List of Figures

Figure 2.1. Molecular structure of solid, liquid crystal and liquid	8
Figure 2.2. Molecular structure of 5CB (4-n-pentyl-4-cyanobiphenyl).	9
Figure 2.3. Status change of a thermotropic liquid crystals.	9
Figure 2.4. Molecular order in a nematic liquid crystal.	10
Figure 2.5. The arrangement of molecules in the cholesteric mesophase.	11
Figure 2.6. The arrangement of molecules in the Smetic A and Smetic C phases	12
Figure 2.7. Polymeric liquid crystals: (a) main chain; (b) side chain.	13
Figure 2.8. The three basic types of deformation in the liquid crystals	14
Figure 2.9. The Freedericksz-transition. Left: the condition when the applied voltage is below the threshold value; right: the condition when the applied voltage is above the threshold.	15
Figure 2.10. The force necessary to slide the top plate over the bottom plate with the liquid crystal in between depends on the orientation of the liquid crystal molecules. As a consequence, liquid crystals possess more than one viscosity constant	16
Figure 3.1. Light transmission from an isotropic to anisotropic medium.	30
Figure 3.2. Light transmission and reflection by an anisotropic plate sandwiched between isotropic media.	35
Figure 4.1. Textures realized in the bistable cholesteric display	41
Figure 4.2. Bistable textures of the SSFLC display	42
Figure 4.3. Textures and transitions in the Berreman's bistable twisted nematic	43
Figure 4.4. Flexoelectrically controlled nematic device using surface bistable states	43
Figure 4.5. Bistable surface anchoring in the ZBD device. (a) High tilt defect-free state; (b) Low tilt state (the pair of defects is located in the gray regions)	44
Figure 4.6. Textures and transitions in the <i>BiNem</i> device	45
Figure 5.1. Structure of blue phases {as schematically illustrated in ref. [11a]}.	
a) Double twist cylinder visualizing the local director field. The director (pseudo-vector indicating the preferred orientation of the molecular long axes) is vertical at the central axis of the cylinder and twists continuously along any radial direction.	
b) Arrangement of double twist cylinders in the body-centered cubic unit cell of BPI (space group O^8) and the simple cubic unit cell of BPII (space group O^2), respectively. c) Appearance of disclination lines in the BPI and BPII unit cells.	

- Singularities of the director field (disclinations) appear since the double twist cylinders cannot fill the space of the unit cell continuously. At positions in the vicinity of the disclination lines, the orientational order parameter disappears (as in the isotropic phase). Thus, blue phases are stable in the temperature range close to the isotropic liquid state. 49
- Figure 5.2. a) BP single crystal in a polarizing microscope. b) Kossel diagram (diffraction pattern of a single crystal illuminated by convergent monochromatic light). c) Prof. Dr. Walter Kossel (1888–1956), who studied the diffraction of X-rays on single crystals when the X-ray source is inside the crystal [8].d) Electro-optical test cell showing the electric-field-induced shift of the Bragg wavelength for a BP system with negative dielectric anisotropy.[10]. 51
- Figure 5.3. Compounds used in ref. [1] . 1: Nematic bimesogens ($n=7, 9, \text{ and } 11$). 2: Chiral dopant (R corresponds to mesogenic moieties not being specified in ref. [1]). 52
- Figure 6.1. Rubbing of the polyimide layer. 60
- Figure 6.2. The definition of parameters associated with rubbing. 61
- Figure 6.3. Different pretilt angle generation in photoalignment method 62
- Figure 6.4. (a) Schematic diagram of the stripe patterns with alternating random-planar- and homeotropic-alignment potentials. (b) Director configuration of the YZ and X states. 63
- Figure 6.5. Two types of configurations of bistable LC cells: (a) twisted-homogeneous bistable mode; and (b) bistable hybrid mode. 64
- Figure 6.6. (a) Experimental setup for periodic stripe pattern formation using unpolarized UV light. (b) Schematic illustration of the textured stripe patterns with alternating random-planar- and homeotropic-alignment states after unpolarized UV light exposure. 65
- Figure 6.7. (a) Optical arrangement and coordinate system of the extinction angle method. (b) Polarized light axis related to the director in the extinction angle method. 67
- Figure 6.8. Optical system of the transmission ellipsometer. 67
- Figure 6.9. Polarized microphotographs of the twisted-homogeneous bistable cell using different LCs: (a) MBBA without electric-field application; (b) MBBA with electric-field application; (c) 5CB without electric-field application; and (d) ZLI-2293 without electric-field application. 69
- Figure 6.10. Polarized microphotographs of the bistable HAN cell using different LCs: (a) MBBA without electric-field application; (b) MBBA with electric-

field application; and (c) ZLI-2293 without electric-field application.	70
Figure 6.11. Δ & Ψ on 0 deg incident.	71
Figure 6.12. Δ & Ψ on 30 deg incident.	72
Figure 6.13. Switching behavior of the twisted-homogeneous bistable cell.	73
Figure 6.14. 40 μm pitch LC cell	74
Figure 6.15. 4 μm pitch LC cell	74
Figure 6.16. 1 μm pitch LC cell	74
Figure 7.1. Schematic of SOITE method.	80
Figure 7.2. The cross section of the model of LC cell used to measure the surface polar anchoring energy coefficient.	83
Figure 7.3. Typical POM textures of blue phases observed on cooling (1 $^{\circ}\text{C}/\text{min}$): BP I.	84
Figure 7.4. Optical system of transmission ellipsometer.	84
Figure 7.5. Digital camera image of the LC cell under voltage application.	85
Figure 7.6. Δ^+ and Δ^- under applied voltage.	86
Figure 7.7. $\Delta^- - \Delta^+$ under applied voltage.	86
Figure 8.1. Geometry of an HAN cell.	93
Figure 8.2. Schematic diagram of light passing through an HAN cell for the oblique incidence. The xz plane is assumed to be the plane of incidence.	95
Figure 8.3. The cross section of the model of LC cell used to measure the surface polar anchoring strength.	97
Figure 8.4. AFM image of bar coated substrate – 2D.	98
Figure 8.5. AFM image of bar coated substrate – 3D.	98
Figure 8.6. Typical POM textures of blue phases observed on cooling (1 $^{\circ}\text{C}/\text{min}$): (a) BP II, (b) BP I, and (c) N*.	99
Figure 8.7. Refractive indices of 5CB + JC-1041XX.	100
Figure 8.8. Relationship of capacitance versus applied voltage.	101
Figure 8.9. Theoretical and experimental results of R versus λ for $\beta = 0^{\circ}$.	102
Figure 8.10. Theoretical and experimental results of R versus β for $\lambda = 440, 550$ and 600 nm.	102

List of Tables

Table 4.1. Comparison of the performances of the main liquid crystal technologies	47
Table 6.1. Twist angle measurement results	71
Table 6.2. Elastic constant K ratio of the LC materials	71
Table 7.1. Composition of LC mixture.	79
Table 7.2. Composition of samples used in the alignment film (Mixture 1).	79
Table 7.3. The properties of ZLI-4792.	83
Table 7.4. The experimental result.	87
Table 8.1. Composition of LC mixture.	91
Table 8.2. Composition of samples used in the alignment film (Mixture 2).	91
Table 8.3. Measurement values of refractive indices of 5CB +JC-1041XX obtained by using Abbe refractometer.	100
Table 8.4. The simulated results of initial values of Cauchy coefficients of anisotropic refractive indices.	100
Table 8.5. LC device parameters of 5CB + JC-1041XX determined by capacitance measurement.	101

Chapter 1

Introduction

1.1. History of Liquid Crystals

Between 1850 and 1888, researchers in different fields such as chemistry, biology, medicine and physics found that several materials behaved strangely at temperatures near their melting points. It was observed that the optical properties of these materials changed discontinuously with increasing temperatures. W. Heintz, for example, reported in 1850 that stearin melted from a solid to a cloudy liquid at 52°C, changed at 58°C to an opaque and at 62.5°C to a clear liquid. He and a colleague, at one point referred to the change at 62.5°C as a second melting point.

An important invention of the time was the heating stage microscope by Otto Lehmann, a physicist from Karlsruhe, Germany [1]. This microscope allowed control of the temperature of the sample. In a later version, with polarizers added, it became the standard equipment in every liquid crystal research laboratory.

In 1888, an Austrian botanist named Friedrich Reinitzer, interested in the biological function of cholesterol in plants, was looking at the melting behaviour of an organic substance related to cholesterol [2]. (The chemical structure of cholesterol was still unknown. Today we know that the observed substance was cholesteryl benzoate). He observed, as W. Heintz did with stearin 38 years before, that the substance melted to a cloudy liquid at 145.5°C and became a clear liquid at 178.5°C. He also described some of the same color phenomena that had been reported by earlier scientist working with cholesterol derivatives: a blue color briefly appears upon cooling when the clear liquid turns cloudy, and a blue-violet color occurs just before the cloudy liquid crystallizes.

Reinitzer knew of the work of Lehmann and saw the connection between his own observations and Lehmann's findings. He therefore sent some of these samples to Otto Lehman, who at this time was a professor of natural philosophy (physics) in Germany. Lehmann was performed many experiments on this substance with his heating stage microscope. Lehmann described Reinitzer's substance along with substances he received from other investigators in a variety of ways during this time of period. First he called them soft crystals that were almost fluid; then the term "floating crystals" was used, which was later replaced with "crystalline fluids". He gradually became

convinced that the cloudy liquid was a uniform fluid phase, but one that effected polarized light in a manner typical of solid crystals, not liquids. This combination of characteristics – flow properties like liquid and optical properties like a solid – finally led Lehmann to label these substances “liquid crystals”.

Research in the area of liquid crystals burgeoned in the years after 1888. Some of the more important results are listed below:

- 1922: George Friedel describes the structure and properties of liquid crystals and classified them in 3 types (nematics, smectics and cholesterics) [3].
- 1962: The first major English language publication on the subject "*Molecular Structure and Properties of Liquid Crystals*", by Dr. George W. Gray [4].
- 1962: Richard Williams of RCA found that liquid crystals had some interesting electro-optic characteristics and he realized an electro-optical effect by generating stripe-patterns in a thin layer of liquid crystal material by the application of a voltage. This effect is based on an electro-hydrodynamic instability forming what is now called “Williams domains” inside the liquid crystal [5].
- 1964: George H. Heilmeyer, then working in the RCA laboratories on the effect discovered by Williams realized the switching of colors by field-induced realignment of dichroic dyes in a homeotropically oriented liquid crystal. Practical problems with this new electro-optical effect made Heilmeyer to continue work on scattering effects in liquid crystals and finally the realization of the first operational liquid crystal display based on what he called the *dynamic scattering mode* (DSM) [6][7][8].
- 1960s: Pioneering work on liquid crystals was undertaken in the late 1960s by the UK's Royal Radar Establishment at Malvern. The team at RRE supported ongoing work by George Gray and his team at the University of Hull who ultimately discovered the cyanobiphenyl liquid crystals (which had correct stability and temperature properties for application in LCDs).
- 1970: The twisted nematic field effect in liquid crystals was filed for patent by Hoffmann-LaRoche in Switzerland with Wolfgang Helfrich and Martin Schadt listed as inventors. Hoffmann-La Roche then licensed the invention to the Swiss manufacturer Brown, Boveri & Cie who produced displays for wrist watches during the 1970s and also to Japanese electronics industry which soon produced the first digital quartz wrist watches with TN-LCDs and numerous other products.

- 1971: The company of Fergason ILIXCO (now LXD Incorporated) produced the first LCDs based on the TN-effect, which soon superseded the poor-quality DSM types due to improvements of lower operating voltages and lower power consumption.
- 1972: The first active-matrix liquid crystal display panel was produced in the United States by T. Peter Brody [9].
- 1991: A French theoretical physicist, Pierre-Gilles de Gennes, who had interest to liquid crystals and soon found fascinating analogies between liquid crystals and superconductors as well as magnetic material was rewarded with the Nobel Prize in Physics 1991.

The future of liquid crystals has just begun. There are still unsolved physical problems in this area, despite the fact that researchers in the fifties had already withdrawn from this area, thus giving an interesting field for the pure scientist. The need for liquid crystal applications grew, requiring engineers specialized in this field. Statistics show that cathode ray tube displays in TVs and computer monitors will be overtaken by liquid crystal displays in the near future. More recent applications involve switchable windows that can be changed from clear and opaque with the flip of a switch, liquid crystal displays with wider viewing angles, and displays that can remain in use for years without the need of power.

Knowledge in the field of liquid crystals is crucial for an understanding of biological membranes, thus biologists, medical researchers and pharmacists are also interested in liquid crystal research.

1.2. Research Background

The liquid crystal display (LCD) technology is currently the dominating technology for flat panel displays. The application range from simple twisted nematic (TN) display in a wrist watches to the latest vertically aligned (VA) and in-plane switching (IPS) modes for states of the art, high definition large screen LCD-TVs. The main advantages of the LCD are its thin profile, low emissive display, does not generate any light itself, instead it modulates light passing through the unit. Several mechanisms for light modulation have been developed and presented. These mechanisms include polarization rotation, phase retardation, absorption, light scattering and Bragg reflection.

The photoalignment technology for the alignment of liquid crystal molecules has

lately gathered much attention because of its advantages over the conventional rubbing of polyimide coating and several different approaches for the realization of photoalignment have been presented. Common to all methods is that anisotropy in the alignment layer is provided by exposing linearly polarized ultraviolet (LPUV) light to a photo-sensitive material. Due to its non-contact nature, a photoalignment eliminates generation of dust and electrostatic charges as well as mechanical damage to the surface. From another point of view, photoalignment is also interesting because the technology enables greater control of several important liquid crystal cell parameters, including pretilt angle, azimuthal and polar anchoring energy, all critical parameters for the realization of surface controlled bistable devices.

Portable electronic devices, such as a mobile phones and personal digital assistants, have lately increased the demand for high performance display with low power consumption. An interesting candidate with the potential of fulfilling these demands is the reflective single-polarizer surface controlled bistable twisted nematic (BTN) LCD. Being a direct-view reflective display ambient light is used to read the information. Hence the device does not require any backlight, leading to reduced power consumption and panel weight stable states in the absence of an electric field, is capable of practically unlimited multiplexing, leading to high resolution on a passive matrix. This results in the elimination of the costly active matrix thin film transistor addressing technique that traditionally has to be used in the order to achieve high levels of complexity of the display. Furthermore, in bistable devices, voltage is only needed when the image is changed. As a consequence, the power consumption of these devices is extremely low. Since the early 1980s, nematic, cholesteric and smetic bistable liquid crystal technologies have been proposed. During recent years, there has been an increasing interest in surface controlled bistable nematic device based on anchoring breaking. The main advantage of these newer technologies is their robust and longterm bistability. The bistable LC display is also suitable for portable electric device such as electronic paper (e-paper).

Recently, blue phase (BP) liquid crystal (LC) has attracted the attention of many researchers because of its exotic structures and properties. The BP with a structure of self-assembled three-dimensional cubics formed by double-twisted arranged LC cylinders is usually observed in the cooling process from the isotropic to the chiral nematic (N^*) phase LC [10]. Such a molecular arrangement exhibits an optical isotropy, selective reflection to circular polarized light, a reflective band switched by external fields, and microsecond response. These characteristics show some potential applications of BP such as large-screen flat panel displays and tuneable photonic band

gap materials [11–14]. The very narrow stable temperature range of the BP, however, typically a few Kelvin, is a serious problem for device applications [15]. Although, much effort has been made to expand the narrow temperature range of the BP, Kikuchi *et al.* firstly reported that the temperature range of the BP can be expanded over 60 °C by adding a small quantity of precursor polymers within the BP materials, referred to as a polymer-stabilized blue phase (PSBP) [16]. Coles and Pivenko reported that, in dimer LCs with large flexoelectricity, the temperature range of the BP was more than 44 °C [17]. Yoshizawa and coworkers reported that the T-shaped molecules and the binaphthyl derivative represented the BP temperature ranges of 13 and 29 °C, respectively [18, 19]. Some other methods such as adding hydrogen-bond LCs and nanoparticle stabilization have also been used to expand the BP temperature range [20, 21].

1.3. Objectives of the Investigation

There are two main objectives of the investigation. The first one is to come up with a bistable liquid crystal device using unpolarized UV light, single-step laser patterning on a photoalignment layer using a photomask was proposed to achieve an equilibrium configuration of LC molecules in contact with a periodically patterned substrate. The patterns were formed by stripes of alternating random planar and homeotropic anchoring on a submicrometer scale in the order of 0.5 micrometer. Two possible configurations of bistable LC cells that can be obtained by combining a micropatterned surface formed with alternating random-planar- and homeotropic-alignment with planar- or homeotropic-alignment surfaces were proposed. The alignment properties of the two proposed models were investigated, along with the microscopic switching behavior of micropatterned nematic liquid crystal cells.

The second objective is to investigate the characteristic and properties of polymer-stabilized blue phase. The quantitative evaluation of a coupling coefficient between the blue phase liquid crystal and the diacrylate type polymer, which is to be the framework or the defect line of the polymer-stabilized BPLC is an important subject. In this study, as a coupling coefficient, the polar anchoring strength between the BPLC and the diacrylate type polymer was evaluated by means of the oblique incidence transmission spectroscopic ellipsometry by using SOITE method and Hung's method.

1.4. Outline of This Thesis

Chapter 1 presents the background of alignment of liquid crystals to gain historical perspective of an odyssey of liquid crystals and objectives of this thesis. Chapter 2 deals with consideration of physical properties of liquid crystal. Chapter 3 deals with optics of liquid crystal. Chapter 4 present the bistable liquid crystal technologies. Chapter 5. present the liquid crystalline blue phase. Our new findings are reported in Chapter 6, 7 and 8. Chapter 6 present the investigation of liquid crystal alignment on patterned-alignment films processed by UV light. Two types of configuration of bistable LC cells were proposed and studied. Chapter 7 and Chapter 8 are concerned with polymer –stabilized blue phase. In Chapter 7, the polar anchoring strength for polymer stabilized blue phase LC devices were determined by SOITE method. In Chapter 8, the polar anchoring strength for polymer stabilized blue phase LC devices were determined by Hung’s method. The final conclusion are presented in Chapter 9.

References

- [1] O. Lehmann, *Z. Phys. Chem.* **4** (1889) 462.
- [2] F. Reinitzer, *Wiener Monatschr Für Chem.* **9** (1888) 421.
- [3] G. Friedel, *Annu. Physique* **18** (1922) 273.
- [4] G. W. Gray, S.M. Kelly, *J. Mater. Chem.* **9** (1999) 2037.
- [5] R. Williams, *J. Phys. Chem.* **39** (1963) 382.
- [6] J. A. Castellano, *American Scientist* **94** (2006) 438.
- [7] G. H. Heilmeier and L. A. Zanoni, *Appl. Phys. Lett.* **13** (1968) 91.
- [8] G. H. Heilmeier, L. A. Zanoni and L. A. Barton, *Proc. IEEE* **56** (1968) 1162.
- [9] T. P. Brody, *Information Display* **13** (1997) 28.
- [10] H. Kikuchi: *Struct. Bonding* **128** (2008)
- [11] Z. Ge, S. Gauza, M. Jiao, H. Xianyu, and S. T. Wu: *Appl. Phys. Lett.* **94** (2009) 101104. F. C. Frank, *Disc. Faraday Soc.* **25** (1958) 19.
- [12] S. Y. Lu and L. C. Chien: *Opt. Lett.* **35** (2010) 562. M. Miesowicz, *Nature* **17** (1935) 261
- [13] H. Y. Liu, C. T. Wang, C. Y. Hsu, T. H. Lin, and J. H. Liu: *Appl. Phys. Lett.* **96** (2010) 121103.
- [14] W. Cao, A. Munoz, P. Palfy-Muhoray, and B. Taheri: *Nat. Mater.* **1** (2002) 111.
- [15] Y. Hisakado, H. Kikuchi, T. Nagamura, and T. Kajiyama: *Adv. Mater.* **17** (2005) 96.
- [16] H. Kikuchi, M. Yokota, Y. Hisakado, H. Yang, and T. Kajiyama: *Nat. Mater.* **1** (2002) 64.
- [17] H. J. Coles and M. N. Pivnenko: *Nature* **436** (2005) 997.
- [18] A. Yoshizawa, M. Sato, and J. Rokunohe: *J. Mater. Chem.* **15** (2005) 328.
- [19] A. Yoshizawa, Y. Kogawa, K. Kobayashi, Y. Takanishi, and J. Yamamoto: *J. Mater. Chem.* **19** (2009) 5759.
- [20] W. He, G. Pan, Z. Yang, D. Zhao, G. Niu, W. Huang, X. Yuan, J. Guo, H. Cao, and H. Yang: *Adv. Mater.* **21** (2009) 1.
- [21] H. Yoshida, Y. Tanaka, K. Kawamoto, H. Kubo, T. Tsuda, A. Fujii, S. Kuwababata, H. Kikuchi, and M. Ozaki: *Appl. Phys. Express* **2** (2009) 121501.

Chapter 2

Physical Properties of Liquid Crystals

2.1. Introduction

Most substances can exist in more than one phase. For example, water is a solid below 0°C , a liquid between 0°C and 100°C , and a gas over 100°C . These three phases are different from each other since the molecules in each phase possess different amount of order. In solids, the molecules are constrained to occupy only certain positions. This condition is described by saying that the solid phase possesses positional order. It is also possible for the solid phase to possess orientational order, where the molecules in the specific positions are constrained in the way they orient themselves with respect to one another. When a solid melts to a liquid, both types of order are completely lost. However, for some specific materials there exists an intermediate phase between the solid and the liquid phases, see Figure 2.1. This phase is called liquid crystal phase and is characterized by some degree of long-range order.

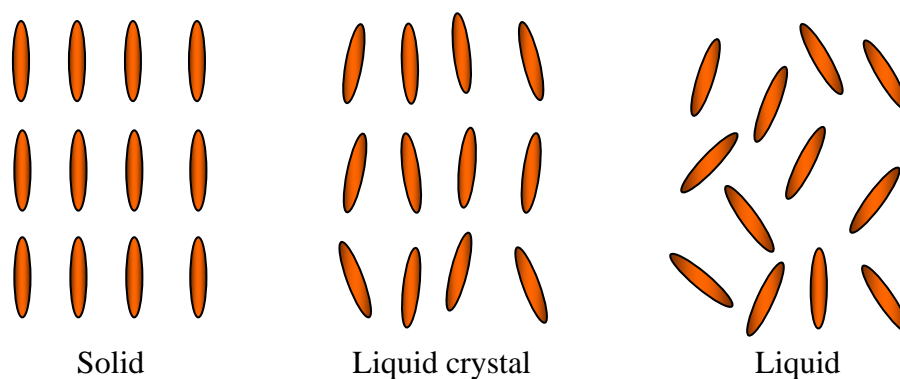


Figure 2.1. Molecular structure of solid, liquid crystal and liquid

Liquid crystal materials generally have several common characteristics. Among these are rod-like molecular structures, rigidity of the long axis, and strong dipoles and/or easily polarizable substituents. The distinguishing characteristic of the liquid crystalline state is the tendency of the molecules (mesogens) to point along a common axis, called the director. This is in contrast to molecules in the liquid phase, which have no intrinsic order. In the solid state, molecules are highly ordered and have little translational freedom. The characteristic orientational order of the liquid crystal state is

between the traditional solid and liquid phases and this is the origin of the term mesogenic state, used synonymously with liquid crystal state. Figure 2.1 shows the average alignment of the molecules for each phase.

In the simplest liquid crystal phase, the nematic phase, the rod-like molecules possess a certain degree of oriental order. One example of material possessing the nematic liquid crystal phase is the low mass cyanobiphenyl 5CB (4-n-pentyl-4-cyanobiphenly) is shown in Figure 2.2.

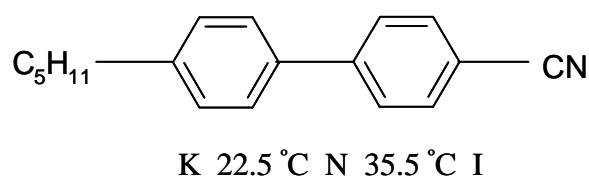


Figure 2.2. Molecular structure of 5CB (4-n-pentyl-4-cyanobiphenly).

2.2. Thermotropic, Polymeric and Lyotropic Liquid Crystals

There are three distinct types of liquid crystals: thermotropic, polymeric and lyotropic. These materials exhibit liquid crystalline properties as a function of different parameters.

2.2.1. Thermotropic Liquid Crystals

In a thermotropic liquid crystals, as the temperature is increased, the solid will lose regularity in position but not in orientation. Thus it has some partial regular structure. Liquid crystals are characterized by regular orientations.

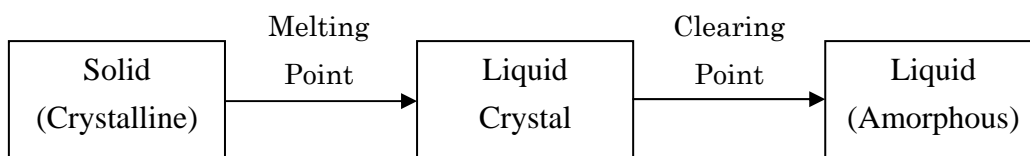


Figure 2.3. Status change of a thermotropic liquid crystals.

There are three phases of liquid crystals. They are nematic, smectic and cholesteric. All common liquid crystal displays are nematic phase. In nematic phase, all the liquid crystal molecules point in the same direction. The spatial position is random. In smectic phase, the liquid crystal molecules point in the same direction as in nematic but there is

some degree of spatial ordering and there is a layer structure. In cholesteric phase, the liquid crystal molecules are same as chiral nematic. The orientation is regular and the spatial position is random.

2.2.1.1. Nematic and Cholesteric Phases

The nematic phase type exists in two well-known structure types: the ordinary nematic structure of nonchiral compounds, and the cholesteric (twisted nematic) structure of substances with chiral molecules.

In the most simple LC phase, one molecular axis tends to point along a preferred direction as the molecules undergo diffusion. This preferred direction is called the director and is denoted by the unit vector \mathbf{n} [1, 2]. An orientational distribution function $f(\theta)d\theta$ can be defined by either taking a snapshot of the molecules at any one time and noting how many axes make an angle θ and $\theta + d\theta$ with the director or by following a single molecule, noting at specific times the angle θ between the molecular axis and the director. Since all directions perpendicular to the director are equivalent in the most simple LC phase, the orientational distribution function does not depend on the azimuthal angle ϕ . A snapshot of elongated molecules in such a phase is shown in Figure 2.4. To specify the amount of orientational order in such a LC phase, an order parameter is defined. This can be done in many ways, but the most useful formulation is to find the average of the second Legendre polynomial,

$$S = \frac{1}{2} \langle 3 \cos^2 \theta - 1 \rangle \quad (2.1)$$

where the brackets denotes an average over many molecules at the same time or the average over time for a single molecules.

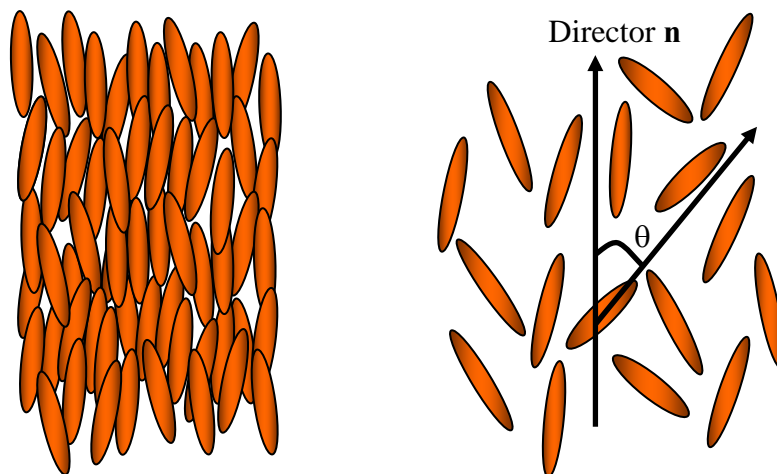


Figure 2.4. Molecular order in a nematic liquid crystal.

The ordinary nematic structure shows an optically positive uniaxial behavior. Chiral molecules cause a twist in the nematic structure, and the cholesteric structure (Figure. 2.5) appears. It consists of a set of quasi-nematic layers, whose individual directors are turned through a fixed angle on proceeding from one layer to the next. The layers which are turned through an angle of 2π are equivalent; their distance defines the pitch p of the screw.

The nematic and the cholesteric phases are very similar in their basic structures. Due to the strong twisting, however, the optical properties of the nematic phase are radically altered. In a certain spectral range, cholesteric phases show a selective reflection of circularly polarized light. The maximum of this reflection lies at the wavelength λ_{\max} :

$$\lambda_{\max} = p \cdot \bar{n} \quad (2.2)$$

\bar{n} is an average refractive index of one quasi-nematic layer.

The cholesteric medium exhibits a strong optical activity which shows a positive as well as negative extreme, and which changes its sign at λ_{\max} . The selective reflection as well as the optical activity remarkably influence the optical appearance (textures) of cholesteric phases, which show optically negative uniaxial behavior.

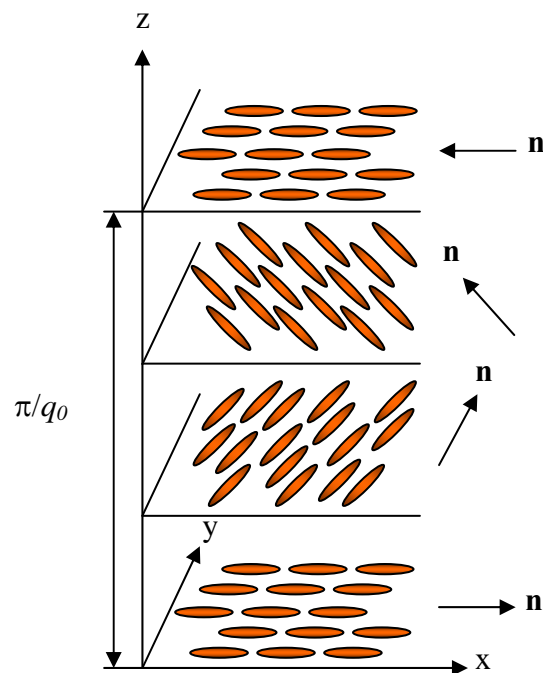


Figure 2.5. The arrangement of molecules in the cholesteric mesophase.

2.2.1.2. Smetic A and Smetic C Phases

In layered liquid crystal phases, there exists both orientational order and some degree of positional order. This layered structure can be observed in the smetic phases. These phases are liquids in two dimensions along the layers but solids in the third dimension. In the smetic A phase, the director is parallel to the layer normal, while in the smetic C phase, the director makes an angle to the normal. This is illustrated in Figure 2.6.

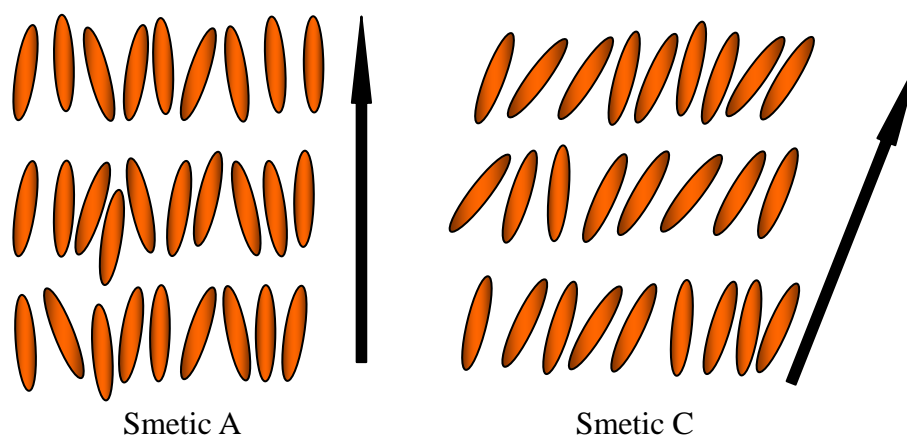


Figure 2.6. The arrangement of molecules in the Smetic A and Smetic C phases

2.2.2. Polymer Liquid Crystals

Polymer liquid crystals (PLCs) are a class of materials that combine the properties of polymers with those of liquid crystals. These "hybrids" show the same mesophases characteristic of ordinary liquid crystals, yet retain many of the useful and versatile properties of polymers.

In order for normally flexible polymers to display liquid crystal characteristics, rod-like or disk-like elements (called mesogens) must be incorporated into their chains. The placement of the mesogens plays a large role in determining the type of PLC that is formed. Main-chain polymer liquid crystals or MC-PLCs are formed when the mesogens are themselves part of the main chain of a polymer. Conversely, side chain polymer liquid crystals or SC-PLCs are formed when the mesogens are connected as side chains to the polymer by a flexible "bridge" (called the spacer.). Figure 2.7. shows the main chain and side chain of polymeric liquid crystals.

Other factors influencing the mesomorphic behavior of polymers include the presence of long flexible spacers, a low molecular weight, and regular alternation of rigid and flexible units along the main chain.

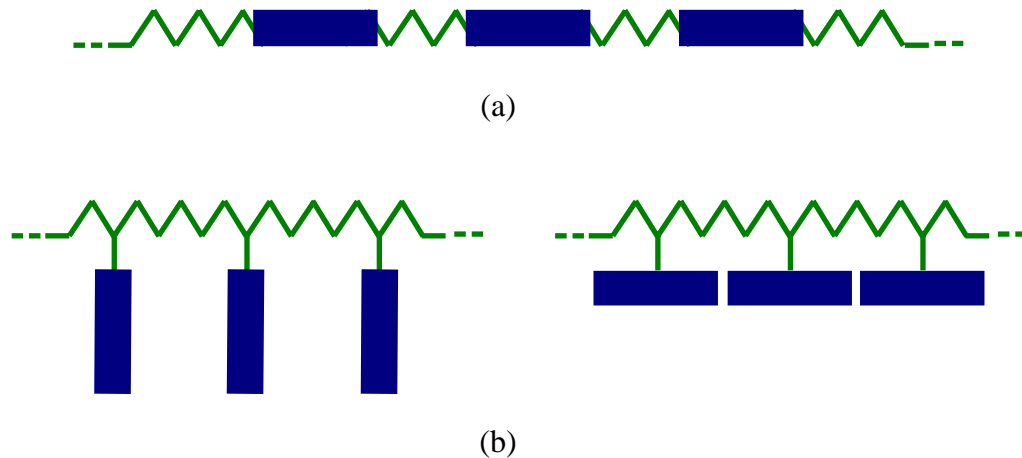


Figure 2.7. Polymeric liquid crystals: (a) main chain; (b) side chain.

2.3. Properties of Liquid Crystals

2.3.1. Dielectric Constant

As a consequence of the orientational order, the nematic liquid crystals are uniaxially symmetric, with the symmetry axis parallel to the long axis of the molecules. This symmetry will lead to different dielectric constants parallel (ϵ_{\parallel}) and perpendicular ϵ_{\perp} to the director. The dielectric anisotropy is defined as

$$\Delta\epsilon = \epsilon_{\parallel} - \epsilon_{\perp}. \quad (2.3)$$

The dielectric anisotropy can be both positive and negative and varies between typical values from $+25\epsilon_0$ to $-5\epsilon_0$, where ϵ_0 is the permittivity of free space. In electro-optical applications of liquid crystals, an electric field is applied to control the orientation of the liquid crystal molecules. Liquid crystals with positive dielectric anisotropy tend to align parallel to the field while liquid crystals with negative dielectric anisotropy align perpendicular. Although liquid crystals with positive dielectric anisotropy are most commonly used, both types can be found in applications depending on the switching principle. If low switching voltage is desired, the liquid crystal used should have large absolute value of the dielectric anisotropy.

Most nematics (e.g., E7, 5CB, etc., $\epsilon_{\parallel} > \epsilon_{\perp}$) are said to possess positive (dielectric) anisotropy. On the other hand, some nematics, such as MBBA, possess negative anisotropy (i.e., $\epsilon_{\perp} > \epsilon_{\parallel}$).

2.3.2. Refractive Index

The uniaxial symmetry also leads to an optical anisotropy (or birefringence) with two principal refractive indices. These two are the ordinary (n_o) and the extraordinary (n_e) index of refraction, for light with its polarization perpendicular and parallel to the director, respectively. Similar to the dielectric anisotropy, the optical anisotropy is defined as

$$\Delta n = n_e - n_o = n_{\parallel} - n_{\perp}. \quad (2.4)$$

and is positive if $n_o < n_e$, while it is said to be negative if $n_o > n_e$. Most liquid crystals with rod-like molecular shape exhibit positive birefringence with typical values ranging from 0.06 up to 0.4.

2.3.3. Elastic Constants

The elastic constants of liquid crystals are the material parameters that determine the restoring torque that arises when the system is perturbed from its equilibrium configuration. When an electric field is applied to reorient the molecules to control the effective birefringence in an electro-optical device, it is the balance between the electric and elastic torque that determines the static deformation of the liquid crystal director. Any deformation can be divided into a combination of three basic deformations, splay, twist and bend. All illustrated is Figure 2.8.

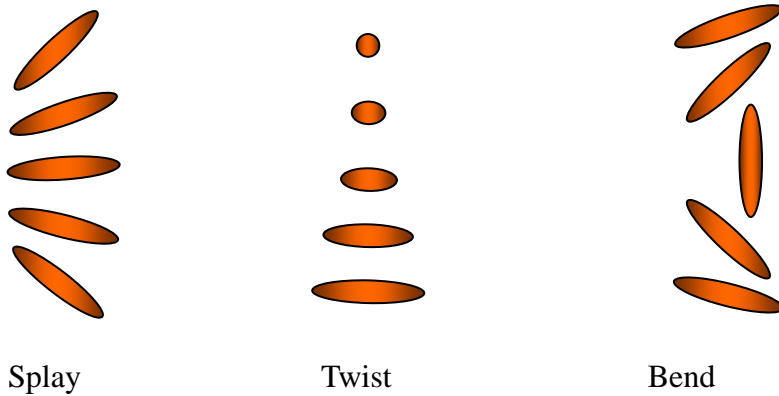


Figure 2.8. The three basic types of deformation in the liquid crystals

According to the notation of the Oseen-Frank theory, the elastic energy density of a deformed nematic liquid crystal can be written [3,4].

$$f_{\text{elas}} = \frac{1}{2} \left[K_{11} (\text{div } \mathbf{n})^2 + K_{22} (\mathbf{n} \cdot \text{curl } \mathbf{n} + q_0)^2 + K_{33} (\mathbf{n} \times \text{curl } \mathbf{n})^2 \right] \quad (2.5)$$

where K_{11} , K_{22} , and K_{33} are the splay, twist and bend elastic constants, respectively. And

$q_0 = \frac{2\pi}{p}$ is the wave vector of a cholesteric.

The positive and negative q_0 values correspond to the right- and left-handed helices, respectively. In ordinary nematic phases, p is infinite, and q_0 therefore vanishes in equation (2.5).

Equation (2.5) is the basis for the theoretical treatment of defects and textures of nematic and cholesteric phases. For a stable distortion, the solutions of equation (2.5) have to yield a relative minimum in the free energy. Distortions that do not correspond to minima of f_{elas} are unstable and should therefore not occur in stable textures.

The minimum voltage needed to reorient the liquid crystal molecules arranged in a parallel untwisted structure as shown in Figure 2.9 is related to the elastic constants as well as to the dielectric anisotropy according to

$$V_c = \pi \sqrt{\frac{K_{11}}{\epsilon_0 \Delta\epsilon}} \quad (2.6)$$

For voltages below the minimum voltage, the liquid crystals remain completely undeformed. Then at some threshold value of the voltage, the deformation begins and gets greater as the voltage increases. This transition from an undeformed to a deformed texture at a certain value is called the Fredericksz-transition [5]. It should be emphasized that strong anchoring to the boundaries prevails and that the director in the undeformed configuration is oriented perpendicular to the electric field.

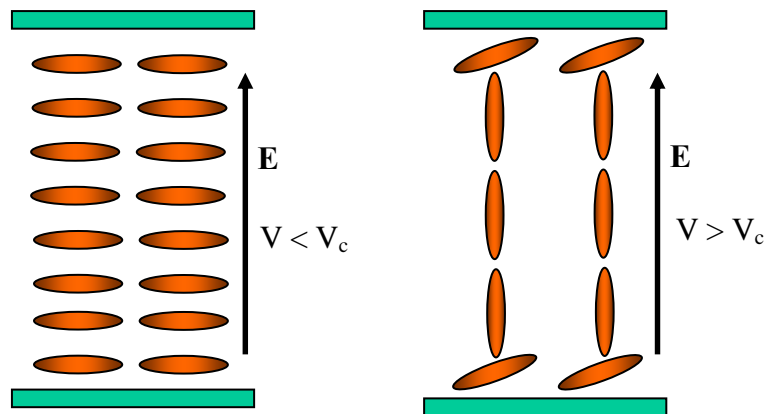


Figure 2.9. The Fredericksz-transition. Left: the condition when the applied voltage is below the threshold value; right: the condition when the applied voltage is above the

threshold.

2.3.4. Viscosity

In the nematic phase the three flow viscosities, η_a , η_b and η_c , also called Miesowicz viscosities [6], can be identified as shown in Figure 2.10. By forcing the director to keep the orientations and moving the top plate, the different viscosities can be measured. As expected, $\eta_c > \eta_a > \eta_b$, that is, that is, when the director is perpendicular to the flow the viscosity is at its largest. If the director is not held in its place, it will be affected by a torque, creating a hydrodynamic torque and introducing two rotational viscosities γ_1 and γ_2 . In most LCDs, the director is reoriented by the application of an electric field. Out of the discussed liquid crystal material parameters, it is mainly the rotational viscosity that defines the switching times.

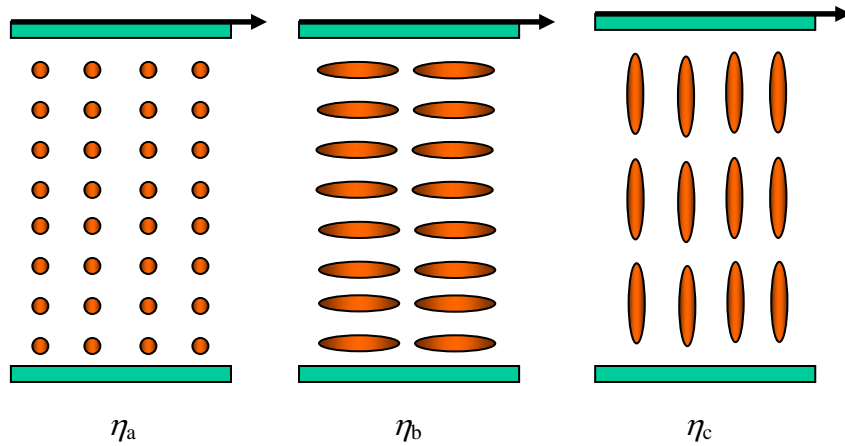


Figure 2.10. The force necessary to slide the top plate over the bottom plate with the liquid crystal in between depends on the orientation of the liquid crystal molecules. As a consequence, liquid crystals possess more than one viscosity constant

$$\tau_{off} \propto \frac{\gamma_{eff} d^2}{K_{eff}} \quad (2.7)$$

$$\tau_{on} \propto \frac{\gamma_{eff} d^2}{\epsilon_0 \Delta \epsilon V^2} \quad (2.8)$$

Equation (2.7) below is typical of nematic relaxation processes in zero electric field, which is quite important for many technical applications of nematics. It gives an

estimation of the relaxation time, the time it takes for the deformed liquid crystal structure to reach its equilibrium configuration after the electric field is switched off [7]. The corresponding response time, the time for the director to reorient in an applied electric field, is given by Equation (2.8). It contains no elastic terms since those can be neglected if the applied voltage is well over the threshold voltage. In equations γ_{eff} is the effective rotational viscosity and K_{eff} is the effective elastic constant, depending on the LC cell molecule configuration. Usually τ_{off} is longer than τ_{on} since the electric torque is stronger than the elastic torque.

References

- [1] F. C. Frank, Liquid crystals: Proc. Int. Conf., Meeting Date December 3, 1979, (S. Chandrasekhar ed.), Heyden, London, England (1980) 1.
- [2] P. J. Collings and M. Hird, "Introduction to Liquid Crystals: Chemistry and Physics", Taylor and Francis, London (1995)
- [3] C. W. Oseen, Trans. Faraday Soc. **29** (1933) 883.
- [4] F. C. Frank, Disc. Faraday Soc. **25** (1958) 19.
- [5] V. Freedericksz and V. zolina, Trans. Faraday Soc. **29** (1933) 919
- [6] M. Miesowicz, Nature **17** (1935) 261
- [7] K. Tarumi, U. Finkenzeller and B. Schuler, Jpn. J. Appl. Phys. **31** (1992) 2829.

Chapter 3

Optics of Liquid Crystals

3.1. Introduction

The optical properties of multilayered anisotropic media such as LC cells have been studied for a long time. Physical models for the optics of LCs have been developed from the beginning of the century. The optics of cholesteric materials was studied by several authors like Mauguin [1], Oseen [2], and de Vries [3]. In 1941, Jones [4] published a 2×2 matrix method for calculating the optical properties of general multilayered anisotropic media at normal light incidence. 4×4 matrix methods were developed by Smith [5] and Berreman [6], which made the calculation at oblique incidence possible. Jones 2×2 matrix method was further improved by Gharadjedaghi [7] and Yeh [8] to cope with oblique incidence. Later on, other 4×4 matrix methods were developed [9, 10]. These matrix methods allow the calculation of the optical properties of general birefringent multilayers with arbitrary orientation of the index ellipsoid in each layer. This flexibility made the matrix methods very attractive for the computation of LCD optics, since polarizers, retarders and of course the LC-layer itself with the arbitrary optic axis orientation can be treated in a systematic way.

3.2. Light Propagation in an Isotropic Medium

Maxwell's equations in a medium

$$\nabla \times \mathbf{E} = -\frac{\partial \mathbf{B}}{\partial t} \quad (3.1)$$

$$\nabla \times \mathbf{H} = \frac{\partial \mathbf{D}}{\partial t} + \mathbf{j} \quad (3.2)$$

$$\nabla \cdot \mathbf{D} = \rho \quad (3.3)$$

$$\nabla \cdot \mathbf{B} = 0 \quad (3.4)$$

Material equation (linear response is assumed)

$$\mathbf{D} = \varepsilon \mathbf{E} = \varepsilon_0 \varepsilon_s \mathbf{E} \quad (3.5)$$

$$\mathbf{B} = \mu \mathbf{H} = \mu_0 \mu_s \mathbf{H} \quad (3.6)$$

$$\mathbf{j} = \sigma \mathbf{E} \quad (3.7)$$

ε : dielectric constant

ε_0 : dielectric constant of vacuum

ε_s : relative dielectric constant (specific inductive capacity)

μ : magnetic permeability

μ_0 : magnetic permeability of vacuum

μ_s : relative magnetic permeability

σ : conductivity

From equations (3.1), (3.2), (3.3), (3.4),

$$\nabla \times (\nabla \times \mathbf{E}) = -\mu_0 \mu_s \frac{\partial}{\partial t} \nabla \times \mathbf{H} = -\mu_0 \mu_s \left(\varepsilon_0 \varepsilon_s \frac{\partial^2 \mathbf{E}}{\partial t^2} + \sigma \frac{\partial \mathbf{E}}{\partial t} \right).$$

Using the identity $\nabla \times (\nabla \times \mathbf{E}) = \nabla (\nabla \cdot \mathbf{E}) - \nabla^2 \mathbf{E}$, and assuming $\rho = 0$, we obtain

$$\nabla^2 \mathbf{E} - \sigma \mu_0 \mu_s \frac{\partial \mathbf{E}}{\partial t} - \varepsilon_0 \varepsilon_s \mu_0 \mu_s \frac{\partial^2 \mathbf{E}}{\partial t^2} = 0 \quad (3.8)$$

because $\nabla \cdot \mathbf{E} = 0$. In the same manner, we obtain

$$\nabla^2 \mathbf{H} - \sigma \mu_0 \mu_s \frac{\partial \mathbf{H}}{\partial t} - \varepsilon_0 \varepsilon_s \mu_0 \mu_s \frac{\partial^2 \mathbf{H}}{\partial t^2} = 0 \quad (3.9)$$

Let us consider a monochromatic plane wave propagating along z direction. Putting

$$E_x = E_0 \exp \left\{ -i\omega \left(t - \frac{z}{v} \right) \right\} \quad (3.10)$$

and substituting this equation into equation (2.50), we obtain

$$\frac{1}{v^2} = \mu_0 \mu_s \left(\varepsilon_0 \varepsilon_s + \frac{i\sigma}{\omega} \right) = \frac{\mu_s}{c^2} \left(\varepsilon_s + \frac{i\sigma}{\omega \varepsilon_0} \right) \quad (3.11)$$

where we use the relation $\varepsilon_0\mu_0 = 1/c^2$ (c : velocity of light in vacuum).

We define the complex refractive index n^* as

$$n^* = \frac{c}{v} = \left\{ \mu_s \left(\varepsilon_s + \frac{i\sigma}{\omega\varepsilon_0} \right) \right\}^{1/2}. \quad (3.12)$$

In $n^* = n + i\kappa$, n is called refractive index and κ is called extinction coefficient.

$$n^2 - \kappa^2 = \mu_s \varepsilon_s, \quad 2n\kappa = \frac{\sigma\mu_s}{\omega\varepsilon_0} \quad (3.13)$$

For nonmagnetic materials, we can put $\mu_s = 1$. In this case, complex relative dielectric constant $\varepsilon_s^* = \varepsilon_1 + i\varepsilon_2$ is given by

$$\varepsilon_1 = n^2 - \kappa^2, \quad \varepsilon_2 = \frac{\sigma}{\omega\varepsilon_0} = 2n\kappa. \quad (3.14)$$

By using n^* , equation (3.10) reduces to

$$E_x = E_0 \exp \left\{ -i\omega \left(t - \frac{nz}{c} \right) \right\} \exp \left(-\frac{\omega\kappa z}{c} \right). \quad (3.15)$$

Equation (3.15) shows that the amplitude of electric field of the light propagating along z direction attenuates exponentially with attenuation coefficient $\omega\kappa/c$.

The absorption coefficient α is defined by

$$\alpha = - \left(\frac{dI}{dz} \right) / I \quad (3.16)$$

where I is the light intensity. From equation (3.16), $I = I_0 \exp(-\alpha z)$. As $I \propto |E_x|^2$,

$$\alpha = 2 \frac{\omega\kappa}{c} = \frac{\omega}{nc} \varepsilon_2 = \frac{1}{nc} \frac{\sigma}{\varepsilon_0}. \quad (3.17)$$

In general, the monochromatic plane wave propagating along the direction defined by unit vector \mathbf{a} is expressed by

$$\mathbf{E} = \mathbf{E}_0 \exp \left\{ -i\omega \left(t - \frac{\mathbf{a} \cdot \mathbf{r}}{v} \right) \right\},$$

$$\mathbf{D} = \mathbf{D}_0 \exp \left\{ -i\omega \left(t - \frac{\mathbf{a} \cdot \mathbf{r}}{v} \right) \right\},$$

$$\begin{aligned}\mathbf{H} &= \mathbf{H}_0 \exp \left\{ -i\omega \left(t - \frac{\mathbf{a} \cdot \mathbf{r}}{v} \right) \right\}, \\ \mathbf{B} &= \mathbf{B}_0 \exp \left\{ -i\omega \left(t - \frac{\mathbf{a} \cdot \mathbf{r}}{v} \right) \right\}.\end{aligned}\quad (3.18)$$

The phase τ of the plane wave is given by

$$\tau = -\omega \left(t - \frac{\mathbf{a} \cdot \mathbf{r}}{v} \right) = \frac{\omega n^*}{c} \mathbf{a} \cdot \mathbf{r} - \omega t = \mathbf{k} \cdot \mathbf{r} - \omega t \quad (3.19)$$

where $k = \frac{\omega n^*}{c}$: (complex) wave number, $k\mathbf{a} = \mathbf{k}$: (complex) wave vector.

3.3. Light propagation in an anisotropic medium

In this case, ε in equation (3.5) becomes tensor, and \mathbf{E} and \mathbf{D} are no longer parallel to each other in general.

$$\mathbf{D} = \boldsymbol{\varepsilon} \mathbf{E} \quad (3.20)$$

or

$$\begin{bmatrix} D_x \\ D_y \\ D_z \end{bmatrix} = \begin{bmatrix} \varepsilon_{xx} & \varepsilon_{xy} & \varepsilon_{xz} \\ \varepsilon_{yx} & \varepsilon_{yy} & \varepsilon_{yz} \\ \varepsilon_{zx} & \varepsilon_{zy} & \varepsilon_{zz} \end{bmatrix} \begin{bmatrix} E_x \\ E_y \\ E_z \end{bmatrix}$$

By using the principle of the conservative of energy, we can show that $\varepsilon_{ij} = \varepsilon_{ji}$, i.e., $\boldsymbol{\varepsilon}$ is a symmetric tensor. Therefore, the coordinate system exists where $\boldsymbol{\varepsilon}$ can be diagonalized as

$$\boldsymbol{\varepsilon} = \begin{bmatrix} \varepsilon_1 & 0 & 0 \\ 0 & \varepsilon_2 & 0 \\ 0 & 0 & \varepsilon_3 \end{bmatrix}.$$

The coordinate axes in this coordinate system are called electric principal axes (or optical principal axes).

In an anisotropic medium, the phase velocity of light, and then, refractive index n depend on the propagation direction of the plane wave. We substitute

$$\begin{aligned} \mathbf{E} &= \mathbf{E}_0 \exp \{ i (\mathbf{k} \cdot \mathbf{r} - \omega t) \} \\ \mathbf{D} &= \mathbf{D}_0 \exp \{ i (\mathbf{k} \cdot \mathbf{r} - \omega t) \} \\ \mathbf{H} &= \mathbf{H}_0 \exp \{ i (\mathbf{k} \cdot \mathbf{r} - \omega t) \} \\ \mathbf{B} &= \mathbf{B}_0 \exp \{ i (\mathbf{k} \cdot \mathbf{r} - \omega t) \} \end{aligned} \quad (3.21)$$

into Maxwell's equations (3.1), (3.2), (3.3) and (3.4) (we assume $\rho = \mathbf{j} = 0$, $\mu_s = 1$), then, we obtain

$$\mathbf{k} \times \mathbf{E} = \omega \mu_0 \mathbf{H}, \quad (3.22)$$

$$\mathbf{k} \times \mathbf{H} = -\omega \mathbf{D}, \quad (3.23)$$

$$\mathbf{k} \cdot \mathbf{D} = 0, \quad (3.24)$$

$$\mathbf{k} \cdot \mathbf{H} = 0. \quad (3.25)$$

From equations (3.23), (3.24), and (3.25), it is easily seen that \mathbf{k} , \mathbf{D} and \mathbf{H} are perpendicular to each other. However, \mathbf{E} is not necessarily perpendicular to \mathbf{k} . From equation (3.22), it is seen that \mathbf{E} is not perpendicular to \mathbf{H} , *i.e.*, it is in the plane made by \mathbf{k} and \mathbf{D} . Then it is understood that the direction of the Poynting vector $\mathbf{S} = \mathbf{E} \times \mathbf{H}$ does not coincide with the direction of \mathbf{k} in general. In other words, the propagation direction of energy does not necessarily coincide with that of the phase in the case of light propagation in an anisotropic medium.

From equations (3.22) and (3.23), we obtain

$$\mathbf{D} = -\frac{1}{\omega} \mathbf{k} \times \mathbf{H} = -\frac{1}{\omega^2 \mu_0} \mathbf{k} \times (\mathbf{k} \times \mathbf{E}) = -\frac{1}{\omega^2 \mu_0} \{ \mathbf{k} (\mathbf{k} \cdot \mathbf{E}) - k^2 \mathbf{E} \}. \quad (3.26)$$

Substituting the relation (see equation (3.19) and $n^* = n$ on the assumption of non-absorbing medium)

$$\mathbf{k} = \frac{\omega}{c} n \mathbf{a} \quad (3.27)$$

into equation (3.26), we obtain

$$\mathbf{D} = -\frac{n^2}{c^2 \mu_0} \{ \mathbf{a} (\mathbf{a} \cdot \mathbf{E}) - \mathbf{E} \} = -n^2 \varepsilon_0 \{ \mathbf{a} (\mathbf{a} \cdot \mathbf{E}) - \mathbf{E} \}. \quad (3.28)$$

In the electric principal axes coordinate system, $E_x = D_x/\varepsilon_1$, $E_y = D_y/\varepsilon_2$, and $E_z = D_z/\varepsilon_3$, then, equation (3.28) can be written as

$$\begin{aligned} D_x \left(\frac{1}{n^2 \varepsilon_0} - \frac{1}{\varepsilon_1} \right) &= -a_x (\mathbf{a} \cdot \mathbf{E}), \\ D_y \left(\frac{1}{n^2 \varepsilon_0} - \frac{1}{\varepsilon_2} \right) &= -a_y (\mathbf{a} \cdot \mathbf{E}), \\ D_z \left(\frac{1}{n^2 \varepsilon_0} - \frac{1}{\varepsilon_3} \right) &= -a_z (\mathbf{a} \cdot \mathbf{E}). \end{aligned} \quad (3.29)$$

From equation (3.24), $\mathbf{a} \cdot \mathbf{D} = a_x D_x + a_y D_y + a_z D_z = 0$. Then, from equation (3.29), we obtain

$$\frac{a_x^2}{\frac{1}{n^2 \varepsilon_0} - \frac{1}{\varepsilon_1}} + \frac{a_y^2}{\frac{1}{n^2 \varepsilon_0} - \frac{1}{\varepsilon_2}} + \frac{a_z^2}{\frac{1}{n^2 \varepsilon_0} - \frac{1}{\varepsilon_3}} = 0. \quad (3.30)$$

If we put

$$\begin{aligned} c_1 &= \frac{1}{\sqrt{\varepsilon_1 \mu_0}} = \frac{1}{\sqrt{\varepsilon_0 \mu_0}} \sqrt{\frac{\varepsilon_0}{\varepsilon_1}} = \frac{c}{\sqrt{\varepsilon_{s1}}} \\ c_2 &= \frac{1}{\sqrt{\varepsilon_2 \mu_0}} = \frac{1}{\sqrt{\varepsilon_0 \mu_0}} \sqrt{\frac{\varepsilon_0}{\varepsilon_2}} = \frac{c}{\sqrt{\varepsilon_{s2}}} \\ c_3 &= \frac{1}{\sqrt{\varepsilon_3 \mu_0}} = \frac{1}{\sqrt{\varepsilon_0 \mu_0}} \sqrt{\frac{\varepsilon_0}{\varepsilon_3}} = \frac{c}{\sqrt{\varepsilon_{s3}}} \\ c_n &= \frac{c}{n} \end{aligned} \quad (3.31)$$

Equation (3.30) reduces to

$$\frac{a_x^2}{c_n^2 - c_1^2} + \frac{a_y^2}{c_n^2 - c_2^2} + \frac{a_z^2}{c_n^2 - c_3^2} = 0. \quad (3.32)$$

Equation (3.32) can be written as

$$(c_n^2 - c_2^2)(c_n^2 - c_3^2)a_x^2 + (c_n^2 - c_3^2)(c_n^2 - c_1^2)a_y^2 + (c_n^2 - c_1^2)(c_n^2 - c_2^2)a_z^2 = 0. \quad (3.33)$$

c_1 , c_2 and c_3 are called principal propagating velocities, and

$$\begin{aligned} n_1 &= c/c_1 = \sqrt{\varepsilon_{s1}}, \\ n_2 &= c/c_2 = \sqrt{\varepsilon_{s2}}, \\ n_3 &= c/c_3 = \sqrt{\varepsilon_{s3}}, \end{aligned} \quad (3.34)$$

are called principal refractive indices. Equation (3.32) or (3.33) is the Fresnel's equation of wave normal, which gives the phase velocity c_n and the refractive index of the light wave whose wave normal propagates along \mathbf{a} direction. Equation (3.33) is a quadratic equation in c_n^2 . Thus to every direction \mathbf{a} there corresponds two phase velocities c_n . (The two values $\pm c_n$ corresponding to any value of c_n^2 are counted as one, since the negative value evidently belongs to the opposite direction of propagation $-\mathbf{a}$.)

For cubic crystal, as $\varepsilon_1 = \varepsilon_2 = \varepsilon_3 = \varepsilon$, $\mathbf{D} \square \mathbf{E}$ and the refractive index n is constant irrespective of the propagation direction of light wave.